Optimized Multi-Stage Constant Current Charging Strategy for Li-ion Batteries

Tahir, Muhammad Usman; Sangwongwanich, Ariya; Stroe, Daniel-Ioan; Blaabjerg, Frede

Published in:
Proceedings of the 2023 25th European Conference on Power Electronics and Applications (EPE'23 ECCE Europe)

DOI (link to publication from Publisher):
10.23919/EPE23ECCEEurope58414.2023.10264245

Publication date:
2023

Document Version
Accepted author manuscript, peer reviewed version

Optimized Multi-Stage Constant Current Charging Strategy for Li-ion Batteries

Muhammad Usman Tahir, Ariya Sangwongwanich, Daniel-Ioan Stroe, Frede Blaabjerg
Department of Energy, Aalborg University
Aalborg, Denmark
E-Mail: {mut; ars; dis; fbl}@energy.aau.dk
URL: https://www.energy.aau.dk

Keywords

« CC-CV charging », « Electric Vehicle (EV)», « Lithium-ion battery », « Optimization », and « Thermal behavior ».

Abstract

Various methods have been proposed to reduce the charging time of lithium-ion batteries (LIBs). The multi-stage constant current (MSCC) charging technique has gained significant attention as a potential solution among various proposed methods. A study was conducted to investigate the impact of the MSCC charging technique on LIBs. Specifically, this research focused on the MSCC approach that utilizes the state of charge (SOC) as a stage transition criterion during charging. The Taguchi orthogonal arrays (OAs) were employed to identify the optimal charging current for each stage of the MSCC technique. The study explored the implementation of equal and unequal weight strategies to obtain optimal charging patterns. The experimental results were compared to the standard constant current-constant voltage (CC-CV) charging method, where the MSCC approach can effectively reduce charging time. However, the MSCC charging approach leads to a slight increase in temperature compared to the CC-CV method. Additionally, the energy efficiency of the MSCC charging method was 0.5% lower than that of the CC-CV method. Despite this, MSCC charging holds potential for fast electric vehicle (EV) charging applications.

Introduction

Due to environmental concerns, much emphasis has been given to developing renewable energy sources, including solar, wind power, smart grids, electric transportation, hybrid microgrids, etc. Energy storage technologies such as lithium-ion batteries (LIBs) are essential for renewable and long-term solutions to climate change. Compared to lead-acid batteries, LIBs have a better power/energy density, a lower self-discharge rate, and a longer cycle life [1,2]. For electric vehicles (EVs), LIBs are the primary power source. However, the widespread adoption of EVs faces several LIB-related challenges, including a long charging time, limited mileage range, a lack of charging stations, and a high cost of ownership [3]. Building more charging stations, expanding battery capacity, and stationary vehicle-to-vehicle (V2V) charging are possible solutions to these problems. The range anxiety issue can be resolved by expanding LIBs' capacity. However, the key concern to be solved is the required charging time. Typically, LIBs require 8-12 hours to fully charge at home, compared to 2-6 hours for commercial chargers and 15-60 minutes for fast chargers. The charging duration depends on the charger manufacturer and the power rating of the chargers. The primary risk of fast chargers is temperature rise during charging, which has direct implications on thermal runaway and LIB safety. Therefore, the LIB charger is essential for maintaining LIB performance and lifetime in EV applications.

The charging strategy is the subject of research at the moment. Generally, the charging strategies regulate the power/voltage or current during charging. The constant current constant voltage (CCCV) is the widely used charging strategy for commercial LIBs [4,5]. In CCCV, there are two charging stages. 1) Constant current (CC) is the initial stage which is followed by 2) the constant voltage (CV) stage. The constant current (I_{chg}) is applied as recommended by the manufacturer in the CC stage until the voltage of the LIB reaches the predefined voltage limit (V_{max}). The voltage is kept constant at $Vmax$, and the current is decreased to 5% of the C-rate during the CV stage. C-rate is the ratio of the charging current to the LIB's nominal capacity. Additionally, the high charge current for the CCCV charging protocol can cause lithium plating under high state of charge (SOC) levels. Lithium metal will

form on the surface of the anode electrode when the rate of lithium-ion (Li^+) embedding in the anode material's surface exceeds the rate of diffusion within the materials. This phenomenon, known as lithium plating, has an impact on the cycle life and performance of LIBs [6].

Various charging strategies have been proposed to extend the lifetime of LIBs and regulate the occurrence of lithium plating on the anode electrodes. These strategies include boost charging, pulse charging, constant power charging, temperature-controlled charging, current varying charging, and multi-stage constant current (MSCC) charging. Among those methods, MSCC is considered to provide flexibility in the CCCV charging without causing additional burdens on the chargers. Therefore, the MSCC charging strategy is intended to reduce charging time, enhance charging performance, and extend LIB cycle life.

To implement the MSCC charging strategy, three factors must be identified: 1) the number of stages, 2) the criteria for stage transition, and 3) the charging current of each stage [7]. The impact of the number of stages on the performance of the LIB has been investigated in previous research, where it concluded that the performance improves as the number of stages increases from one to five and marginally beyond five [8]. In the literature, four types of transition criteria were employed: 1) SOC-based transition [4,8], 2) Time-based transition [6], 3) Threshold voltage-based transition [9], and 4) Cut-off voltage-based transition [10]. Most of the previous research used an empirical or experimental method instead of a systematic method to find the C-rate for each stage. Typically, the higher C-rate is chosen during the initial stages. When predetermined conditions for stage transition are reached, the charging procedure is changed to subsequent stages with a lower C-rate.

In fact, it is important to maximize the charging energy efficiency and charged/discharged capacity while minimizing the charging time and temperature rise. All the mentioned parameters are considered performance parameters. Some of the performance parameters are contradictory and cannot be easily optimized simultaneously. Therefore, the MSCC charging can be considered an optimization problem. Several optimization methods are employed to determine the optimal charge pattern for LIBs. The previous research utilized the Taguchi method [11], genetic algorithm [12], ant colony system [13], particle swarm optimization [14], grey golf optimization [15], and numerical optimization [16]. The existing studies on the Taguchi method are presented in Table I. In [10, 11, 17, 18], the authors obtained the optimal charge pattern using the orthogonal experiments with the cut-off voltage-based transition to shorten the charging time, improve other performance parameters, and extend the cycle life. In [4], the authors implemented the four-stage constant current charging strategy with equal SOC intervals to find the sub-optimal charge pattern. The results show that the four-stage MSCC charging has a shorter charging time. However, the charging efficiency is lower than the equivalent CCCV method. In [5], the authors applied the four-stage MSCC charging strategy with equal SOC intervals on the lithium polymer batteries to determine the optimal charge pattern. The results demonstrated that the MSCC reduces the charging time with lower temperature variation and slightly higher energy efficiency than the equivalent CCCV method. From the practical perspective, it is not straightforward to find the effect of different C-rate on the performance parameters that reflects the physics-based parameters and models to generalize characteristics for LIBs. In addition, the effect of unequal SOC intervals on the higher C-rate is not yet investigated with the Taguchi method for current optimization. Thus, the impact of the MSCC charging strategy with unequal SOC intervals for lithium-iron-phosphate (LFP) cells is investigated in this article. The effect of the higher C-rate on the charging performance is also discussed in detail.

This work proposed an optimal charging pattern based on the performance parameters for LIBs. The impact of weighting factors on charging patterns was analyzed. The effect of performance parameters on optimal charge patterns is investigated using the equal and unequal weight factor strategy. The paper is divided into five sections. Section II introduces the Taguchi method and its elements for analysis. Section III describes the experimental setup and test procedure in more detail. The results of the experiment are discussed in section IV. The paper is concluded in section V.

Taguchi Optimization Method

The Taguchi technique employs a design of experiments (DOE) strategy to systematically

TABLE I. Existing research papers focused on the Taguchi method for determining the optimal charge pattern.

Ref	Cell Chemistry	Transition Criteria	No. of stages	Max. C-rate	Studied Performance Parameters			
					Charging time	Charged/discharged Capacity	Charging/energy efficiency	Max/avg. Temperature Rise
[4]	Li-ion	Equal SOC Interval	4	1.5	√	√	√	×
[5]	Li-polymer	Equal SOC Interval	4	2	√	√	√	√
[10]	Li-ion	Cut-off Voltage	4	1.4	√	√	√	×
[17]	Li-ion	Cut-off Voltage	4	1.45	√	√	√	√
[11]	Li-ion	Cut-off Voltage	5	2	√	√	√	√
[18]	Li-ion	Cut-off Voltage	5	1.5	√	√	√	√
This work	LFP	Unequal SOC Interval	5	3	√	√	√	√

investigate how different charging parameters affect LIB's performance [11]. By optimizing the design for robustness, it attempts to minimize the effect of variations in the performance parameters. The method analyses the performance data and determines the best parameter values using orthogonal arrays and signal-to-noise (S/N) ratios.

The utilization of the Taguchi method offers numerous advantages in the optimization of LIBs charging. The utilization of this method results in a reduction of the number of experiments required in comparison to test all the possible parameter combinations, thereby saving time and resources. The method enables the optimization of multiple charging parameters simultaneously, taking into account their interactions and impact on battery performance. The Taguchi method ensures consistent and reliable battery performance by achieving robustness in the charging process. This reduces the risk of undercharging, overcharging, or overheating.

The fundamental idea is to produce a minimum sensitivity design that can optimize the output variables despite input variables having random variability within certain limits. The method has the three-phases: 1) system design, 2) parameter design, and 3) tolerance design. The system design is the process of choosing variables for input and outputs. In this case, the C-rate for each stage is considered as an input variable, and outputs are the performance parameters of LIBs. The parameter design phase is the designing of the candidate's current levels for each stage. The last phase is the tolerance design. The tolerance design in this paper for LIB is considered a 0.2C rate. The main goal is to reduce the experimental cost while providing the optimal solution. The orthogonal array and signal-to-noise (S/N) ratio are two essential elements of the Taguchi method for experiment design.

Selection of Orthogonal Array

The orthogonal array experimental design proposed by Taguchi can be used to evaluate the effect of various parameters on the performance characteristic in a compressed set of experiments. Orthogonal arrays (OAs) are used to design orthogonal experiments. Moreover, orthogonal experiments are used to analyze the multi-factor and multi-level experiments. The general OA is represented by $E_n(L^F)$, where n represents the number of experiments, and L and F represent the number of levels and factors, respectively. The suitable orthogonal array can be chosen based on the number of factors and levels. This paper presents a five-stage constant current (5SCC) charging strategy. Therefore, five current stages are considered as factors, each with three current candidates as levels. Thus, eighteen experiments are conducted based on L_{18} OA with five factors and three current levels.

Signal-to-noise ratio

The effect of each current stage with three current candidate levels can be analyzed using the S/N ratio. In the Taguchi method, the S/N ratio is used to find the effect of each factor and level on quality function. The performance parameters are considered quality parameters, and their optimization function is the quality function in this paper. The S/N ratio can be derived as follows:

$$S/N_{fl} = \begin{cases} -10\log\left(\frac{1}{n}\sum_{i=1}^{n}\left(y_{fl}^{2}\right)\right), & STB \\ -10\log\left(\frac{1}{n}\sum_{i=1}^{n}\left(y_{fl}^{-2}\right)\right), & LTB \end{cases} \quad (1)$$

Where n, i, and y_{fl} represent the number of samples, i_{-th} sample, and experimental observations with associated factors and levels, respectively. The Taguchi method utilizes the mean squared deviation concept to calculate the S/N ratio. The S/N ratio is calculated based on STB and LTB. Here, STB means smaller the better type of response, and LTB means larger the better type of response. After the mean effect of the S/N ratio, each factor's effect is calculated by weight strategy to optimize the current level accordingly. The charging time and max/avg temperature rise are considered as STB type response parameters. The energy efficiency and charged capacity are considered LTB-type responses in the quality function.

Experimental Setup

MSCC Charging Strategy

This paper investigated the 5SCC charging strategy with SOC-based transition. An example of the 5SCC charging strategy is illustrated in Fig.1. The charging current of the nth stage is shown as I_n. The current of each stage is steadily decreased and is expressed as follows:

$$I_1 > I_2 > I_3 > I_4 > I_5 > 0 \quad (2)$$

LFP Cell

The key electrical properties of the used LFP battery are listed in Table II. For all experiments, the Neware battery testing station is used. To keep a constant and stable temperature throughout the experiment, the cell is put in the Memmert temperature chamber, as shown in Fig. 2.

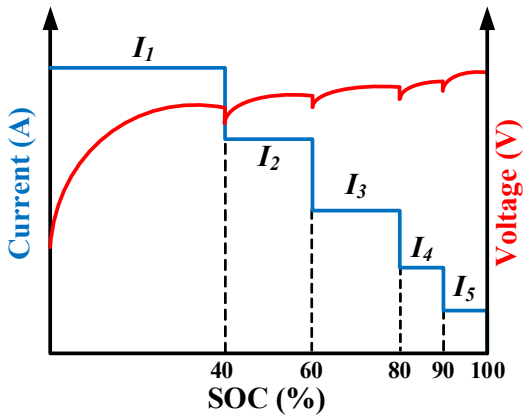

Fig. 1: A illustration of implemented five-stage constant current charging strategy.

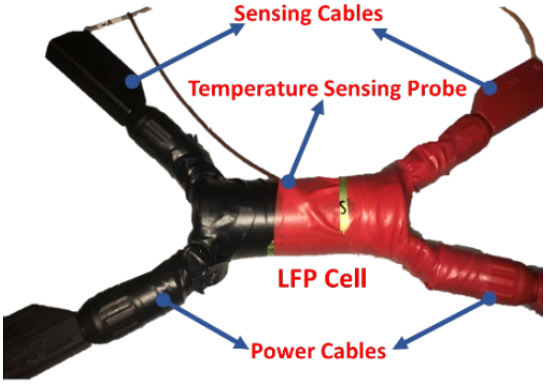

Fig. 2: LFP cell during testing in the temperature chamber.

TABLE II. Key electrical parameters of tested LFP Cell.

Characteristic	Value
Nominal capacity (Ah)	2.6
Nominal voltage (V)	3.3
Cut-off voltage (V)	3.6
Minimum discharge voltage (V)	2
Maximum charge current (A)	10.4
Operating temperature (°C)	-30 – 55
Internal Impedance (1 kHz typical)	6 mΩ

TABLE III. Current candidates for 5SCC charging experiments.

Levels (A)	Factors (Units in C-rate)				
	I_1	I_2	I_3	I_4	I_5
1	3	2.4	1.8	1.2	0.6
2	2.8	2.2	1.6	1	0.4
3	2.6	2	1.4	0.8	0.2

Experimental Design

Multi-factor optimization problems can be solved effectively using the Taguchi method. Firstly, the highest permitted C-rate by the manufacturer until 80% SOC is 4C. To maintain safety and prevent lithium plating, the LIB is charged at a maximum 3C rate. To evenly distribute the charging current at each level, the 3C is divided into fifteen intervals. Though, the difference between the two consecutive levels is 0.2 C. In addition, each current stage (factor) has three levels of charging, which are listed in Table III. Secondly, based on the number of stages and current levels, the suitable OA is selected. The L_{18} has been chosen for a five-stage, three-level

TABLE IV. Illustration of the implemented L_{18} orthogonal array experiments.

Exp. no	S_1	S_2	S_3	S_4	S_5
1	$I_{1,1}$	$I_{2,1}$	$I_{3,1}$	$I_{4,1}$	$I_{5,1}$
2	$I_{1,1}$	$I_{2,2}$	$I_{3,2}$	$I_{4,2}$	$I_{5,2}$
3	$I_{1,1}$	$I_{2,3}$	$I_{3,3}$	$I_{4,3}$	$I_{5,3}$
4	$I_{1,2}$	$I_{2,1}$	$I_{3,1}$	$I_{4,2}$	$I_{5,2}$
5	$I_{1,2}$	$I_{2,2}$	$I_{3,2}$	$I_{4,3}$	$I_{5,3}$
6	$I_{1,2}$	$I_{2,3}$	$I_{3,3}$	$I_{4,1}$	$I_{5,1}$
7	$I_{1,3}$	$I_{2,1}$	$I_{3,2}$	$I_{4,1}$	$I_{5,3}$
8	$I_{1,3}$	$I_{2,2}$	$I_{3,3}$	$I_{4,2}$	$I_{5,1}$
9	$I_{1,3}$	$I_{2,3}$	$I_{3,1}$	$I_{4,3}$	$I_{5,2}$
10	$I_{1,1}$	$I_{2,1}$	$I_{3,3}$	$I_{4,3}$	$I_{5,2}$
11	$I_{1,1}$	$I_{2,2}$	$I_{3,1}$	$I_{4,1}$	$I_{5,3}$
12	$I_{1,1}$	$I_{2,3}$	$I_{3,2}$	$I_{4,2}$	$I_{5,1}$
13	$I_{1,2}$	$I_{2,1}$	$I_{3,2}$	$I_{4,3}$	$I_{5,1}$
14	$I_{1,2}$	$I_{2,2}$	$I_{3,3}$	$I_{4,1}$	$I_{5,2}$
15	$I_{1,2}$	$I_{2,3}$	$I_{3,1}$	$I_{4,2}$	$I_{5,3}$
16	$I_{1,3}$	$I_{2,1}$	$I_{3,3}$	$I_{4,2}$	$I_{5,3}$
17	$I_{1,3}$	$I_{2,2}$	$I_{3,1}$	$I_{4,3}$	$I_{5,1}$
18	$I_{1,3}$	$I_{2,3}$	$I_{3,2}$	$I_{4,1}$	$I_{5,2}$

experiment. The selected OA is represented in Table IV.

Test Procedure

The LFP cell was charged at 25 °C using a 5SCC charging strategy. At a lower level of SOC, the higher charging C-rate will not significantly affect the degradation of the cell's electrode materials [6]. Therefore, the SOC interval for the first stage is set to 0–40% to charge the LIB at a higher C-rate. The LIB is charged to 40–60% of the SOC in the second stage and 60–80% of the SOC in the third stage. Then, the remaining 20% of the SOC is charged in two stages with 10% SOC intervals. All experiments are carried out in accordance with the specified SOC intervals, as shown in Fig. 1. The following is the testing procedure for implementing the MSCC charging strategy:

1. Rest the LIB for one hour at 25°C.
2. Discharge the LIB at 1C current until it reaches the discharge cut-off voltage.
3. Rest the LIB for an hour at 25 °C to stabilize the open circuit voltage (OCV) and eliminate thermal stress.
4. Charge the LIB at the predetermined C-rate for each stage until the SOC interval or 3.6V reaches.
5. Rest the LIB for 1.5 hours at 25 °C to stabilize the OCV and eliminate thermal stress.
6. Discharge the LIB at 1C current until it reaches the discharge cut-off voltage.
7. Rest the LIB for one hour at 25 °C to stabilize the OCV and eliminate thermal stress.
8. Repeat steps 4–7 for each experiment.

Each factor's effect on each level is calculated, indicating the impact of each level on the performance parameters. The optimal charge pattern can be established after using the weight strategy.

TABLE V. Experimental results of studied performance parameters and their S/N ratio.

Ex no.	Observations					S/N Ratios				
	Chg-time (s)	Chg-Cap (Ah)	Eff (%)	Max-Temp (°C)	Avg-Temp (°C)	Chg-time	Chg-Cap	Chg-eff	Max-Temp	Avg-Temp
1	2059	2.5902	93.55	31.20	29.53	-66.273	8.267	39.421	-29.883	-29.404
2	2425	2.5889	94.30	30.70	29.12	-67.694	8.262	39.490	-29.743	-29.283
3	3501	2.5889	94.63	30.60	28.35	-70.884	8.262	39.521	-29.714	-29.052
4	2434	2.5865	94.29	31.20	29.17	-67.726	8.254	39.489	-29.883	-29.299
5	3491	2.5876	94.69	30.70	28.39	-70.859	8.258	39.526	-29.743	-29.062
6	2186	2.5801	94.43	30.40	29.06	-66.793	8.233	39.502	-29.657	-29.266
7	3347	2.5871	94.67	30.60	28.47	-70.493	8.256	39.524	-29.714	-29.086
8	2251	2.579	94.52	30.40	28.90	-67.048	8.229	39.511	-29.657	-29.218
9	2554	2.5832	94.56	30.60	28.83	-68.144	8.243	39.514	-29.714	-29.196
10	2593	2.5825	94.46	30.80	29.00	-68.276	8.241	39.505	-29.771	-29.248
11	3241	2.5855	94.45	31.00	28.69	-70.214	8.251	39.504	-29.827	-29.155
12	2085	2.579	94.27	30.50	29.21	-66.382	8.229	39.487	-29.686	-29.311
13	2269	2.579	94.30	30.90	29.13	-67.117	8.229	39.490	-29.799	-29.286
14	2504	2.5832	94.43	30.60	28.97	-67.973	8.243	39.502	-29.714	-29.240
15	3241	2.5845	94.61	30.80	28.46	-70.214	8.248	39.519	-29.771	-29.085
16	3399	2.5848	94.64	30.60	28.32	-70.627	8.249	39.521	-29.714	-29.041
17	2284	2.5776	94.35	30.80	29.03	-67.174	8.224	39.495	-29.771	-29.257
18	2451	2.5829	94.45	30.40	28.85	-67.787	8.242	39.504	-29.657	-29.202

TABLE VI. Normalized effect of each current level on each performance parameter and weight level calculation for optimized charge pattern.

Response (dB)	Levels	Factors (number of stages)				
		I_1	I_2	I_3	I_4	I_5
Equal Weights	1	0.9989	0.9988	0.9988	0.9996	0.9880
	2	0.9987	0.9991	0.9993	0.9997	0.9953
	3	0.9990	0.9998	0.9990	0.9984	0.9893
Unequal Weights	1	0.9989	0.9987	0.9988	0.9996	0.9925
	2	0.9984	0.9989	0.9991	0.9996	0.9930
	3	0.9986	0.9999	0.9984	0.9975	0.9822

Result and Discussion

The experiments were conducted in line with the experimental design methodology described in Section III. The performance parameters were directly obtained from the observations, and their S/N ratio can be calculated by (1). The smaller the better S/N ratio is calculated for charging time, maximum temperature rise, and average temperature rise, and the larger the better S/N ratio is applied for charging capacity and energy efficiency. Table V illustrates the observations and their S/N ratio, where it can be seen that experiment no. 1 charged the LIB in the shortest amount of time with the highest increase in surface temperature and the lowest energy efficiency, whereas experiment no. 5 charged the LIB in the longest amount of time with the highest efficiency. The temperature variation is based on the first stage charging current, and the temperature is gradually reduced in the following stages. Therefore, it is necessary to optimize the charge pattern.

The next step is calculating the average S/N ratio ($\overline{S/N}_{j,fl}$) of each current level for each stage. Fig. 3 shows the average effect of each current candidate level on each current stage. For the charging time and average temperature rise, the fifth stage has the most significant influence compared to the other stages. At the same time, the charged capacity is decreased as the current increases. The first three stages impact the surface temperature rise more than the later stages. The energy efficiency is decreased as the current increases in each stage. The divergence in Fig. 3 shows the relative effect of current candidates' levels on performance parameters. Thus, the performance parameters are contradictory, and the weight strategy is applied to find the optimal charge pattern.

For finding the optimal charge pattern, the obtained S/N data is normalized using (3).

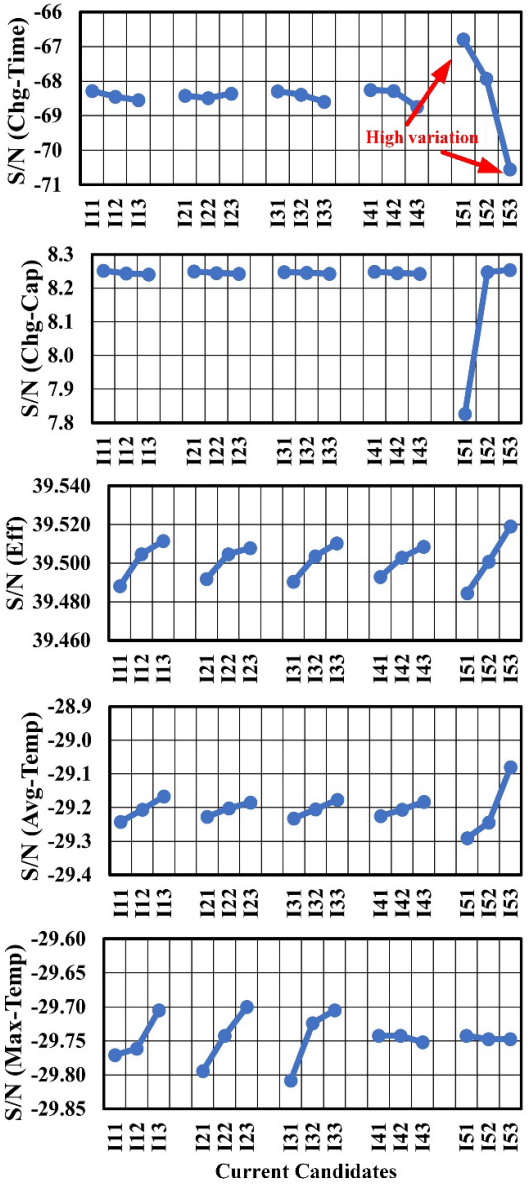

Fig. 3: Average effect of each current level on each performance parameters.

TABLE VII. Comparison of the proposed 5SCC charging with CCCV charging method based on their performance parameters.

Charge Method	Charge Current	Nominal Charge Capacity (%)	Nominal Discharge Capacity (%)	Charge time (Sec)	Energy Efficiency (%)	Pre-set Temp (°C)	Max. Temp. Rise (°C)	Avg. Temp. Rise (°C)
CCCV	1.38 C to 3.6 V and 0.05 C cut-off	100	100	2808	94.4	25.8	4.5	2.1
5SCC (equal weights with an average 1.38 C)	S1 2.6 C S2 2.0 C S3 1.6 C S4 1.0 C S5 0.4 C	99.6	99.8	2604	93.9	25.8	5.4	3.4
CCCV	1.46 C to 3.6 V and 0.05 C cut-off	99.6	100	2601	94.7	25.7	4.5	2.4
5SCC (Unequal weights with an average 1.46 C)	S1 3.0 C S2 2 C S3 1.6 C S4 1.2 C S5 0.4 C	99.4	100	2509	94.2	25.8	5.7	3.8

$$\alpha_{fl} = \begin{cases} \dfrac{max_n(\overline{S/N}_{j,fl})}{\overline{S/N}_{j,fl}}, & STB \\ \dfrac{\overline{S/N}_{j,fl}}{max_n(\overline{S/N}_{j,fl})}, & LTB \end{cases} \quad (3)$$

After normalization, the equal and unequal weight strategies are applied to find the optimal charge pattern. For an equal weight strategy, each performance parameter is weighted as 1. Thus, the average level of each stage is calculated and represented in Table VI. For the unequal weight strategy, the charging time, the max/avg temperature rise, the energy efficiency, and the charged capacity weights are assigned as 3, 2, 2, 1, 1, respectively. The average weight is calculated and illustrated in Table VI.

As seen from Table VI, for equal weight strategy, 2.6C, 2C, 1.6C, 1C, and 0.4C are the optimal charge pattern for stage 1, stage 2, stage 3, stage 4, and stage 5, respectively. In addition, for the unequal weight strategy, 3C, 2C, 1.6C, 1.2C, and 0.4C is the optimal charge pattern for the 5SCC charging strategy.

Comparison with CCCV

The performance parameters by employing the 5SCC charging strategy are compared with the equivalent CCCV method. First, the LIB is charged using the optimal charge pattern as mentioned earlier for both weights' strategies and determined the average C-rate using (4).

$$CC_{avg} = \left[\frac{\sum_{n=1}^{5} I_n \times T_n}{\sum_{n=1}^{5} T_n} \right] \Big/ 2.6 \quad (4)$$

Where CC_{avg} represents the average C-rate for the 5SCC charging strategy and I_n, n, T_n shows the charge current, number of stages, and charging time for each stage, respectively.

The LIB is charged with the average C-rate by employing the equivalent CCCV method. Table VII shows the performance parameters for both weights charging strategies and their equivalent CCCV charging methods. The experimental results show that the 5SCC charging strategy speed up the charging process compared to the equivalent CCCV method, as shown in Fig. 4 (a-b) for both weights strategies. In addition, the maximum temperature rise and the average temperature in the 5SCC charging strategy are higher than the corresponding CCCV technique, as shown in Fig. 4(c). This is because heat generation during the 5SCC charging strategy is higher due to the higher C-rate in the first three stages than CCCV. Also, the effect of temperature is dependent upon Li-ion chemistry. The LFP chemistry is more affected by heat generation during charging than the other chemistries [19]. Furthermore, the energy efficiency of the 5SCC charging strategy is 0.5% lower than the equivalent CCCV charging method. The nominal charged and discharged capacity is approximately the same compared to the CCCV charging method. Moreover, the unequal weight strategy reduced the charging time and improved the

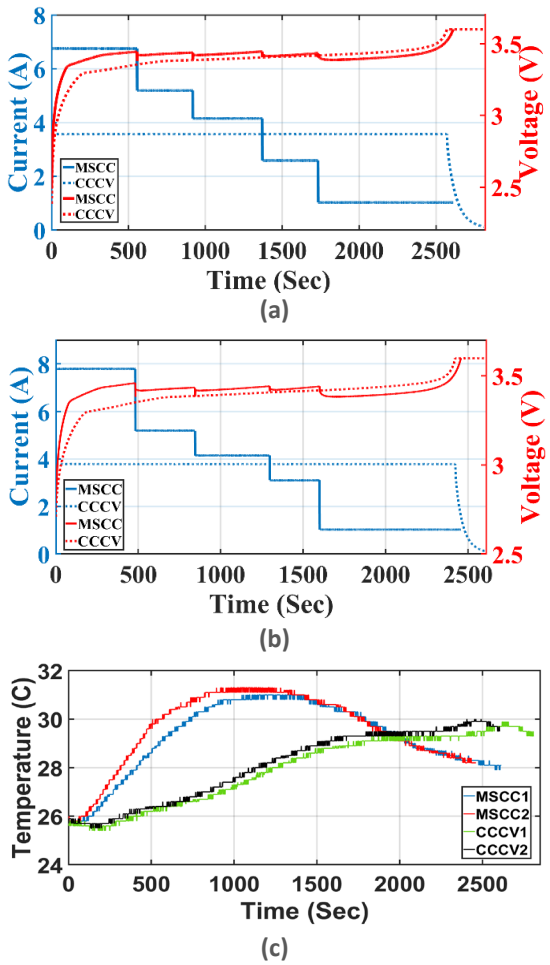

Fig. 4: The optimal MSCC charging strategy is compared to the equivalent CCCV charging method using two different weighting schemes: a) equal weight MSCC charging with CCCV, and b) unequal weight MSCC charging with CCCV. c) Temperature variation in charging techniques (1, 2 represents equal weights strategy and unequal weight strategy respectively).

energy efficiency compared to an equal weight strategy at the cost of a slightly higher surface and average temperature rise.

Conclusion

This study investigates the SOC-based 5SCC charging strategy to reduce the LIB's charging time. The proposed method is integrated with the L_{18} orthogonal array experiment of the Taguchi method to find the optimal charge pattern. The effect of the performance parameters for each stage is analyzed. Furthermore, the weight strategy is applied to find the optimal charge pattern. The performance parameters of the optimal charge pattern are compared to the performance parameters of the corresponding CCCV charging. The result demonstrates that the 5SCC reduces the charging time. The impact on the temperature rise is higher in the 5SCC charging strategy compared to the CCCV charging strategy. In addition, the 5SCC charging method is 0.5% less efficient than the corresponding CCCV charging method. However, the 5SCC charging method can be used for fast EV charging.

Future research will examine the effects of the proposed charging strategy utilizing different lithium-ion chemistries.

References

[1] M. U. Tahir, M. Anees, H. A. Khan, I. Khan, N. Zaffar, and T. Moaz, "Modeling and evaluation of nickel manganese cobalt based Li-ion storage for stationary applications," *J. Energy Storage*, vol. 36, p. 102346, 2021.

[2] M. U. Tahir, T. Moaz, H. A. Khan, N. A. Zaffar, and I. Khan, "Accurate Modeling of Li-ion Cells Applied to LiFePO 4 and NMC Chemistries," *2020 IEEE Texas Power and Energy Conference (TPEC)*, IEEE, 2020, pp. 1–6.

[3] P. Chakraborty *et al.*, "Addressing the range anxiety of battery electric vehicles with charging en route," *Sci Rep*, vol. 12, no. 1, p. 5588, 2022.

[4] C.-H. Lee, M.-Y. Chen, S.-H. Hsu, and J.-A. Jiang, "Implementation of an SOC-based four-stage constant current charger for Li-ion batteries," *J. Energy Storage*, vol. 18, pp. 528–537, 2018.

[5] T. T. Vo, X. Chen, W. Shen, and A. Kapoor, "New charging strategy for lithium-ion batteries based on the integration of Taguchi method and state of charge estimation," *J. Power Sources*, vol. 273, pp. 413–422, 2015.

[6] F. An, R. Zhang, Z. Wei, and P. Li, "Multi-stage constant-current charging protocol for a high-energy-density pouch cell based on a 622NCM/graphite system," *RSC Adv*, vol. 9, no. 37, pp. 21498–21506, 2019.

[7] M. Usman Tahir, A. Sangwongwanich, D.-I. Stroe, and F. Blaabjerg, "Overview of multi-stage charging strategies for Li-ion batteries," *J. Energy Chemistry*, vol. 84, pp. 228–241, 2023.

[8] L.-R. Dung and J.-H. Yen, "ILP-based algorithm for Lithium-ion battery charging profile,"*2010 IEEE International Symposium on Industrial Electronics*, IEEE, 2010, pp. 2286–2291.

[9] M. Dotoli *et al.*, "Development of an Innovative Procedure for Lithium Plating Limitation and Characterization of 18650 Cycle Aged Cells for DCFC Automotive Applications," *Batteries*, vol. 8, no. 8, p. 88, 2022.

[10] C.-H. Lee, T.-W. Chang, S.-H. Hsu, and J.-A. Jiang, "Taguchi-based PSO for searching an optimal four-stage charge pattern of Li-ion batteries," *J. Energy Storage*, vol. 21, pp. 301–309, 2019.

[11] L. Jiang *et al.*, "Optimization of multi-stage constant current charging pattern based on Taguchi method for Li-Ion battery," *Appl. Energy*, vol. 259, p. 114148, 2020.

[12] Y. Li *et al.*, "Optimization of charging strategy for lithium-ion battery packs based on complete battery pack model," *J. Energy Storage*, vol. 37, p. 102466, 2021.

[13] Y.-H. Liu, J.-H. Teng, and Y.-C. Lin, "Search for an optimal rapid charging pattern for lithium-ion batteries using ant colony system algorithm," *IEEE Trans. Ind. Electron.*, vol. 52, no. 5, pp. 1328–1336, 2005.

[14] J. Sun, Q. Ma, C. Tang, T. Wang, T. Jiang, and Y. Tang, "Research on optimization of charging strategy control for aged batteries," *IEEE Trans. Veh. Technol.*, vol. 69, no. 12, pp. 14141–14149, 2020.

[15] G.-J. Chen, Y.-H. Liu, S.-C. Wang, Y.-F. Luo, and Z.-Z. Yang, "Searching for the optimal current pattern based on grey wolf optimizer and equivalent circuit model of Li-ion batteries," *J. Energy Storage*, vol. 33, p. 101933, 2021.

[16] Y. Li, K. Li, Y. Xie, J. Liu, C. Fu, and B. Liu, "Optimized charging of lithium-ion battery for electric vehicles: Adaptive multistage constant current–constant voltage charging strategy," *Renew. Energy*, vol. 146, pp. 2688–2699, 2020.

[17] C.-H. Lee, C.-Y. Hsu, S.-H. Hsu, and J.-A. Jiang, "Effect of Weighting Strategies on Taguchi-Based Optimization of the Four-Stage Constant Current Charge Pattern," *IEEE Trans. Aerosp. Electron. Syst.*, vol. 57, no. 5, pp. 2704–2714, 2021.

[18] Y.-H. Liu and Y.-F. Luo, "Search for an optimal rapid-charging pattern for Li-ion batteries using the Taguchi approach," *IEEE Trans. Ind. Electron.*, vol. 57, no. 12, pp. 3963–3971, 2009.

[19] P. Jindal, R. Katiyar, and J. Bhattacharya, "Evaluation of accuracy for Bernardi equation in estimating heat generation rate for continuous and pulse-discharge protocols in LFP and NMC based Li-ion batteries," *Appl. Therm. Eng.*, vol. 201, p. 117794, 2022.